

TITLE: FRC STUDIES ON FRX-B

AUTHOR(S): W. T. Armstrong, J. C. Cochrane, R. K. Linford,
J. Lipson, A. G. Sgro, E. G. Sherwood, R. E. Siemon,
M. Tuszewski and K. F. McKenna

SUBMITTED TO: Third Symposium on the Physics and Technology
of Compact Toroids

MASTER

DISCLAIMER
This document is the property of the U.S. Government and is loaned to your organization. It and its contents are not to be distributed outside your organization. If you are not an authorized recipient, please notify the nearest office of the U.S. Government Printing Office.

University of California

By acceptance of this article, the publisher recognizes that the U.S. Government retains a nonexclusive, royalty-free license to publish or reproduce the published form of this contribution, or to allow others to do so, for U.S. Government purposes.

The Los Alamos Scientific Laboratory requests that the publisher identify this article as work performed under the auspices of the U.S. Department of Energy.



LOS ALAMOS SCIENTIFIC LABORATORY

Post Office Box 1663 Los Alamos, New Mexico 87545

An Affirmative Action/Equal Opportunity Employer



FRC Studies on FRX-B

W. T. Armstrong, J. C. Cochrane, J. Lipson, R. V. Linford, K. F. McKenna,
A. G. Sgro, E. G. Sherwood, R. E. Siemon, and M. Tuszewski

Introduction

Recent experimental studies of Field-Reversed Configurations (FRC) on the FRX-B¹ device have included 1) characterization of FRC formation with regard to loss of bias flux, 2) examination of FRC equilibria through separatrix profiles, 3) formation of FRC's with different end-mirror configurations, and 4) extension of FRC parameter range. Studies on loss of bias flux during the pre-ionization (PI) phase of FRC formation are presented in another paper dedicated solely to PI considerations.² Loss of bias flux during the reversal phase of FRC formation is reviewed in the first section of this paper. Use of barrier fields during the reversal phase to enhance trapping of bias flux is included in the third section of this paper. In addition to barrier field studies, results from different mirror configurations are also discussed in the third section. A critical diagnostic for interpretation of the results from the different machine modifications is the excluded-flux probe array. Analysis of excluded-flux measurements to obtain the FRC separatrix profile is described in the second section. Finally, preliminary results of FRX-B operation in an extended range of plasma parameters is briefly discussed in the fourth section.

Flux Annihilation during the Reversal Phase

The trapped flux of a FRC is defined by $\phi_1 = \int_0^R B_z 2\pi r dr$ where B_z is the magnetic field in the axial midplane, and R is the radius at which $B_z = 0$. Both experiment and theory suggest that the longest lived FRC's are produced when ϕ_1 is maximized. The largest possible bias flux that can be trapped is $\pi r_t^2 B_{bias} = \phi_0$, where r_t is the inner radius of the discharge tube (10 cm) and B_{bias} is the magnitude of the bias field (~2.4 kG). In past work, the final configuration has $\phi_1/\phi_0 \sim 0.14$.¹ Due to the nature of the PI technique used,^{2,3} $\phi_1/\phi_0 \sim 0.5$ at the initiation of the main bank. During the rise of the main field, flux may be annihilated by resistive processes. We endeavored to examine this last loss mechanism in detail.

The apparatus consists of a theta-pinch coil which has a 22-cm id and is 100 cm in length. The field sequence begins with the slow rise of the negative bias field. A ringing theta-pinch PI is initiated near the bias field maximum such that the net field passes through zero ("zero-crossing PI"²). Finally, the main bank is fired whereupon the field attains its maximum positive value (~15 kG) with a risetime of 2.6 μ s. Data were taken with a radial array of B_z probes located in the axial midplane of the device. The radial probe array also contained coils which were sensitive to toroidal field. However, no toroidal field was observed during the implosion, even when the radial array was moved off the axial midplane.

Figure 1 displays ϕ_1/ϕ_0 vs time for data averaged over five shots taken at a D_2 filling pressure of 17 mtorr. The error bars correspond to shot-to-shot variations. Also plotted in Fig. 1 are the results of a computer simulation of the implosion using a 1-D hybrid code (Vlasov ions, fluid electrons).^{4,5} The model employed either Chodura⁶ or classical resistivity. To account for the observation of current flowing between the sheath and the wall, a hot tenuous plasma created from particles being continuously emitted by the wall was included. In addition, anomalous joule heating of the ions (~50% of the ohmic

heating) was employed. The initial conditions were an electron temperature of 4 eV, 100% ionization, and $\phi_1/\phi_0 = 0.5$. Though the detailed results for the simulation with Chodura resistivity diverge somewhat from the data, the end value of ϕ_1/ϕ_0 is similar. The inadequacy of classical resistivity to recover the final observed ϕ_1/ϕ_0 suggests that the resistivity must be anomalous during this time. There are preliminary indications from the computer simulations that ϕ_1/ϕ_0 evaluated at the peak of the external field is bigger for larger bias fields. Hence, a substantial improvement in ϕ_1 may be possible for operations at larger bias fields.

Separatrix Profile from Analysis of Excluded Flux Measurements

At each of nine stations along the FRX-B coil, the excluded-flux radius $r_{\Delta\phi} = r_p(1 - \phi_p/\pi r_p^2 B_p)^{1/2}$ is obtained with flux loop (ϕ_p) and B_z probe (B_p) data. These diagnostics are located at a radius r_p . The excluded flux radius profile, $r_{\Delta\phi}(z)$, is therefore available over the entire length of the theta-pinch coil. In general, $r_{\Delta\phi}(z)$ differs from the separatrix profile $r_s(z)$. The latter profile is important since it gives the dimensions of the FRC equilibrium. A numerical procedure⁷ has been developed to determine a separatrix profile consistent with the $r_{\Delta\phi}$ data. Plasma pressure on open field lines is neglected and constant flux is assumed at the inner coil surface at a given time.

We give in Fig. 2 numerical analysis results for a typical shot from past experimental data.¹ The separatrix profile (solid line) and the corresponding excluded-flux radius profile (dotted line) are shown in Fig. 2, along with the five experimental values of $r_{\Delta\phi}$ (circles) available from stations on half the coil. In Fig. 2, $r_s(z)$ corresponds to a probable smooth profile. Several separatrices are consistent with the experimental data since, as was shown numerically,⁷ the excluded flux array can only resolve features of the separatrix that have a scale length greater than about a coil radius.

FRC Behavior for Different Barrier and Mirror Field Geometries

Studies of FRC formation have been performed utilizing different barrier and mirror field geometries with a variety of main field amplitudes. Table I briefly summarizes the different configurations and the FRC behavior observed. Referring to Table I, cases (1) and (2) had a solid, main coil (100 cm long with a 25-cm id) which passively produced 10% mirror fields at each end of the coil. Cases (3), (4), and (5) employed an azimuthally-slotted main coil (100 cm long with a 22-cm id) which had no passive mirrors. The coil was slotted to allow application of an octopole barrier field from an azimuthal array of longitudinal conductors. In addition to the slotted main coil and barrier field coils, case (3) also utilized independent mirror coils at both ends of the main coil. These mirror coils produced a peak, on-axis field of ~11 kG during the rise of the main field. Furthermore, a "non-zero-crossing,"² theta-pinch PI was used in cases (2), (3), and (5) where large bias fields (~3.0 kG) complimented the high B_{max} operation. A conventional "zero-crossing"² theta-pinch PI was used with the modest bias field levels (~2.3 kG) in cases (1) and (4). A D_2 fill at 17 mtorr was used in all cases.

Removal of passive mirrors with the installation of barrier coils resulted in FRC's which suffered a rapid decay (10 to 15 μ s lifetimes). End-on framing pictures indicated the configuration was often grossly turbulent and died erratically. The $n=2$ rotational instability was absent. The short plasma lifetime appears to be associated with the production of a "poor" FRC equilibria. Excluded-flux measurements indicate that the FRC equilibrium had a length comparable to the coil length, was irregularly positioned along the axis, and displayed a tendency to move axially. Application of the independent

mirror fields during FRC formation (case(3)) resulted in equilibria more consistently centered in the coil. However, the equilibrium length was still comparable to the coil length and the lifetime was still 10 to 15 μ s.

Though the slotting of the main coil and presence of barrier field coils may contribute to the rapid decay of the FRC, the lack of continuous mirror fields appears to be the most likely cause of the short FRC lifetime. The absence of mirror fields allows longer FRC equilibria. Equilibria with lengths comparable to the length of the coil may have several deleterious effects on the FRC lifetime: 1) field line divergence at the coil ends may induce net axial drifts of the FRC, 2) contact of the FRC with the cold end region may result in rapid cooling leading to annihilation of the FRC, or 3) complete field line reconnection may never occur.

The octopole barrier fields were produced by energizing a set of 16 longitudinal conductors. Connecting the conductors in two different arrangements maximized either the B_r or the B_θ component of the octopole field geometry. Both modes were studied and gave a similar result: a modest increase in the separatrix radius was observed at early times (~10% increase ~5 μ s after the main field initiation was typical). However, the effect of increased excluded-flux radius on late-time FRC behavior was obscured by the short plasma lifetime described above. Use of the barrier field (case (4)) is illustrated in Fig. 3.

Extended FRC Parameter Range

Past scaling studies of FRC parameters employed a bias field of -2.3 kG and maximum main field of ~9 kG (case (1), Table I). These field values and associated conventional PI technique limited the formation of FRC's to a D_2 fill pressure range of 5 to 23 mtorr. Recent studies with a bias field of -3.0 kG, maximum main field of ~13 kG and "non-zero-crossing" PI (case (2), Table I) have extended FRC formation over a range of fill pressure from 5 to 50 mtorr. Similar FRC behavior is observed as in the previous operation: 1) separatrix radius is ~5.5 cm, 2) stable period scales approximately linearly with fill pressure up to ~50 μ s, and 3) $n=2$ rotational instability terminates the FRC. The increase in main field generally increased T_i such that only a modest increase in R/ρ_i is observed (ρ_i is the vacuum ion gyro-radius). The modest increase in stable period over the previous study (~15%) appears consistent with a scaling of stable period with R/ρ_i . Moreover, the stable periods appear to be very insensitive to the rather large increases in T_i at a given R/ρ_i (an increase in T_i of $\times 2.5$ is typical).

References

1. W. T. Armstrong, R. K. Linford, J. Lipson, D. A. Flatts, and E. G. Sherwood, accepted in Phys. Fluids, 1980.
2. R. J. Comisso, W. T. Armstrong, J. C. Cochran, C. A. Ekdahl, J. Lipson, R. K. Linford, E. G. Sherwood, R. E. Siemon, and M. Tuszewski, "The Initial Ionization Stage of FRC Formation," Proceedings of this conference.
3. W. T. Armstrong, J. C. Cochran, R. J. Comisso, J. Lipson, and M. Tuszewski, submitted to App. Phys. Lett., 1980.
4. A. G. Sgro and C. W. Nielsen, Phys. Fluids 19, 126 (1976).
5. A. G. Sgro, Phys. Fluids 23, 1055 (1980).
6. R. Chodura, Nucl. Fusion 15, 55 (1975).
7. M. Tuszewski, submitted to Phys. Fluids, 1980.

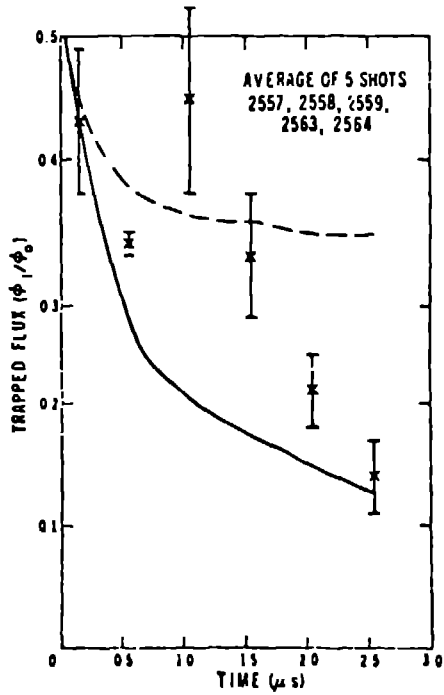


Fig. 1. ϕ_1/ϕ_0 is compared between experiment and simulation during the rise of the main field. The dashed and solid lines represent simulations with classical and Chodura resistivity, respectively.

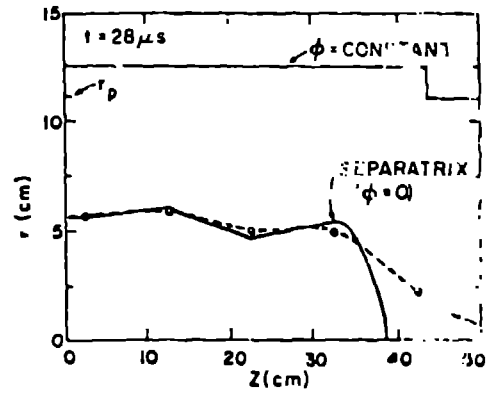


Fig. 2. Measurements of the excluded-flux radius vs z and the associated separatrix profile are compared.

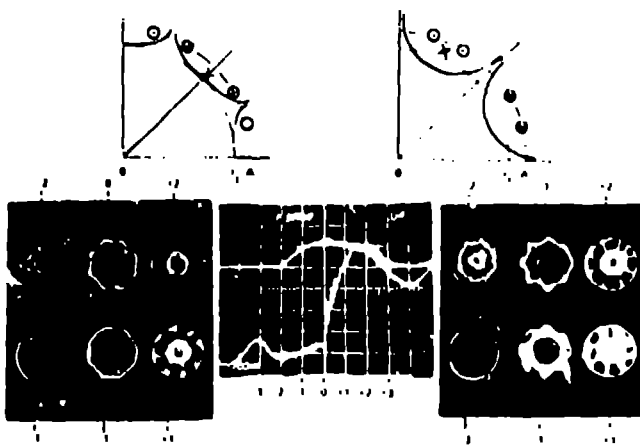


Fig. 3. End-on framing pictures are compared for barrier field operation with maximized B_z (on left) and maximized B_0 (on right). The oscillogram traces are the barrier field (upper) and the main B_z field (lower).

TABLE I
FRX-B OPERATION IN 1980

B_{max}	SHRODS	BARRIER	BEHAVIOR
1. 9 kG (DATA FROM 1979)	PASSIVE	-	LONG-LIVED FRC, n = 2 INSTABILITY
2. 13 kG	PASSIVE	-	LONG LIVED FRC, n = 2 INSTABILITY
3. 15 kG	PULSED	NOT ENERGIZED	RAPID DECAY OF FRC
4. 9 kG	NONE	B_z OR B_0	ϕ_1 INITIALLY INCREASED BUT FRC DECAYED RAPIDLY
5. 15 kG	NONE	B_z	ϕ_1 INITIALLY INCREASED BUT FRC DECAYED RAPIDLY